JOC The Journal of Organic Chemistry

Article

pubs.acs.org/joc

Synthesis and Photophysics of a 2,7-Disubstituted Donor−Acceptor Pyrene Derivative: An Example of the Application of Sequential Ir-Catalyzed C−H Borylation and Substitution Chemistry

Lei Ji, Andreas Lorbach, Robert M. Edkins,* and Todd B. Marder*

Institut für Anorganische Chemie, Julius-Maximilians-Universität Würzburg, Am Hubland, 97074 Würzburg, Germany

Supporting Information

ABSTRACT: We report a general and selective method to synthesize 2,7-disubstituted pyrene derivatives containing two different substituents by sequential Ir-catalyzed borylation and substitution chemistry. To demonstrate the utility of our approach, we synthesized 2-cyano-7-(*N*,*N*-diethylamino)-pyrene (**3**), a pyrene analogue of the widely studied chromophore 4-(*N*,*N*-dimethylamino)benzonitrile (DMABN). Compound **3** and the monosubstituted compounds 2-(*N*,*N*-diethylamino)pyrene (**1**) and 2-cyanopyrene (**2**) have been structurally characterized. Their electronic and optical properties have been studied by a combination of absorption and emission spectroscopies, lifetime and quantum yield measurements, and modeling by DFT and TD-DFT. The photophysical properties of **3** are compared to those of DMABN and 2-cyano-7-(*N*,*N*-dimethylamino)-4,5,9,10-tetrahydropyrene, and we show that 2,7-disubstituted pyrene is a moderately effective π-bridge for the construction of donor−acceptor compounds. It is also shown that donor or acceptor groups are only effective at the 2,7-positions of pyrene if they are suitably strong, leading to a switch in the energetic ordering of the HOMO−1 and HOMO or the LUMO and LUMO+1 of pyrene, respectively.

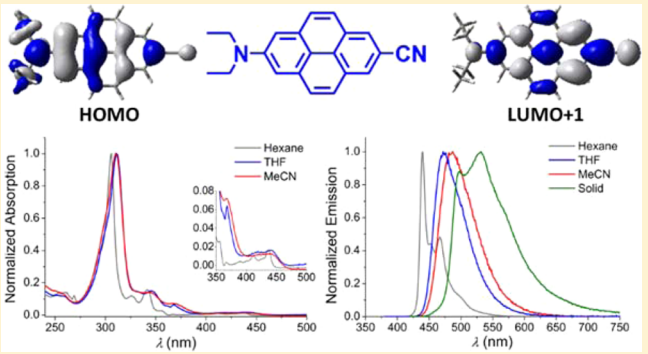

INTRODUCTION

The photophysical properties of pyrene and its derivatives have been investigated extensively, including their often intense and long-lived fluorescence, excimer and exciplex formation, and polarity-dependent emission spectra (Ham effect).[1] Recently, we reported the syntheses[2] and photophysical properties[3] of a diverse series of 2- and 2,7-substituted pyrene derivatives, which were shown to have significant differences in their optical behavior when compared to more typical 1-substituted analogues. The syntheses of these compounds were made feasible by exploiting the selectivity of Ir-catalyzed C−H borylation,[4] which allowed regioselective functionalization at the 2- and 7-positions through steric control.[5] This contrasts with and complements electrophilic aromatic substitution chemistry, which is selective for the 1-, 3-, 6-, and 8-positions, due to large contributions to the HOMO at these sites, whereas a nodal plane in the HOMO coincident with the long axis of pyrene through the 2- and 7-positions makes these sites typically unamenable to electrophilic substitution.[6]

We have further exploited selective borylation of pyrene in the synthesis of a range of functional materials, including pyrene-thienoacene chromophores,[7] cyclometalated iridium complexes,[8] and low-molecular-weight gelators.[9] We have also studied the crystal polymorphism, solvate formation, and cocrystallization of the parent compounds 2-(Bpin)pyrene and 2,7-bis(Bpin)pyrene (pin = pinacolato, $Me_2C(O^-)C(O^-)$-Me_2),[10] and have shown that borylation at the 4-position of pyrene is feasible if both the 2- and 7-positions are blocked by other groups.[11] Finally, we have recently shown that further borylation at the 9- and 10-positions of pyrene is irreversible,[12] in contradiction to earlier claims.[13]

Hence, the ability to functionalize pyrene at the 2- and 7-positions has become firmly established in recent years; however, there is no general method to functionalize pyrene selectively at the 2,7-positions with two different substituents.[6] Such molecules may be of interest for optical and electronic applications, in which the pyrene unit acts as a π-bridge between, for example, an electron acceptor and donor group (as explored here) or between two different redox active centers. Notably, Song and co-workers very recently reported the synthesis of a 2,7-substituted pyrene derivative with a diphenylamino donor and a thienyl acrylic acid acceptor, which they used as a dye in a dye-sensitized solar cell with promising performance (4.1% power conversion efficiency).[14] However, this compound was synthesized from 2,7-dibromopyrene, made according to the method of Harvey and co-workers,[15,16] which itself requires multistep synthesis, namely, hydrogenation of pyrene, iron-catalyzed dibromination, and subsequent reoxidation. Starting from 2,7-dibromopyrene is also not an

Received: March 18, 2015
Published: April 30, 2015

DOI: 10.1021/acs.joc.5b00618
J. Org. Chem. 2015, 80, 5658−5665

inherently selective method for the formation of mono- or disubstituted derivatives; indeed, the $Ni(PPh_3)_2$(1-naphthyl)Cl-catalyzed amination reported by Song afforded the product 2-bromo-7-(*N*,*N*-diphenylamino) in only 10% yield relative to the 2,7-dibromopyrene starting material.[14] Therefore, due to the potential wide utility of the products, we were motivated to develop a protocol that was both more general and selective. Herein, we present a sequential Ir-catalyzed borylation and substitution methodology that fills this gap in the synthetic toolbox for pyrene.

We demonstrate our approach through the synthesis of the compound 2-cyano-7-(*N*,*N*-diethylamino)pyrene (**3**) (Scheme 1), specifically selected because it can be viewed as a pyrene analogue of the extensively studied chromophore 4-(*N*,*N*-dimethylamino)benzonitrile (DMABN). DMABN is a deceptively simple compound, which displays interesting yet complex photophysical behavior.[17−24] This behavior includes dual emission from both a twisted intramolecular charge transfer (TICT) state and a locally excited state, the ratio of which is dependent on solvent polarity, viscosity, and temperature. Thus, it is of interest to make a direct comparison of the photophysical properties of **3** and DMABN, particularly in light of the frontier-orbital structure of the parent compound pyrene in which both the HOMO and LUMO have nodal planes coincident with the long axis of the molecule that might be expected to lead to modulated charge transfer between the donor and acceptor units.

Scheme 1. Molecular Structures of Target Compounds 1−3

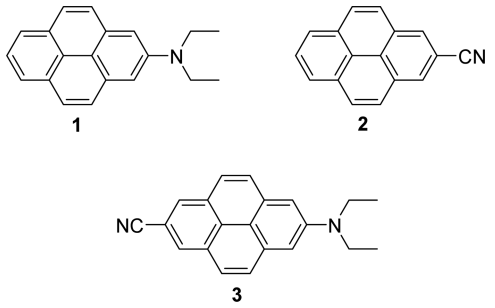

RESULTS AND DISCUSSION

Synthesis. We began with the synthesis of the monosubstituted pyrene derivative 2-(*N*,*N*-diethylamino)pyrene (**1**) (Scheme 2). Following our reported[5] selective monoborylation of pyrene to afford 2-(Bpin)pyrene and conversion of this compound to 2-bromopyrene in high isolated yield,[2] a copper-mediated amination with diethylamine and stoichiometric CuI was attempted; however, no reaction had occurred after 4 days at 80 °C in *N*-methyl-2-pyrrolidone. Instead, **1** was synthesized by Buchwald-Hartwig amination using the precatalyst $Pd_2(dba)_3$ (0.3 mol %; dba = dibenzylideneacetone), the phosphine ligand SPhos (1 mol %; SPhos = 2-dicyclohexylphosphino-2′,6′-dimethoxybiphenyl) and NaO^{t}Bu base. This reaction was complete in 4 h, and **1** could be isolated as a yellow solid in a moderate yield of 30%. Direct *ipso* cyanation of 2-(Bpin)pyrene was performed using an adaptation of the method developed by Hartwig and co-workers,[25] affording 2-cyanopyrene (**2**) in a yield of 45%. Ir-catalyzed C−H borylation of 2-bromopyrene gave 2-Bpin-7-bromopyrene (**4**) in 52% yield. This compound has the potential to serve as a valuable intermediate in the synthesis of a wide range of 2,7-disubstituted pyrene derivatives bearing two different sub-

Scheme 2. Syntheses of Compounds 1−5[a]

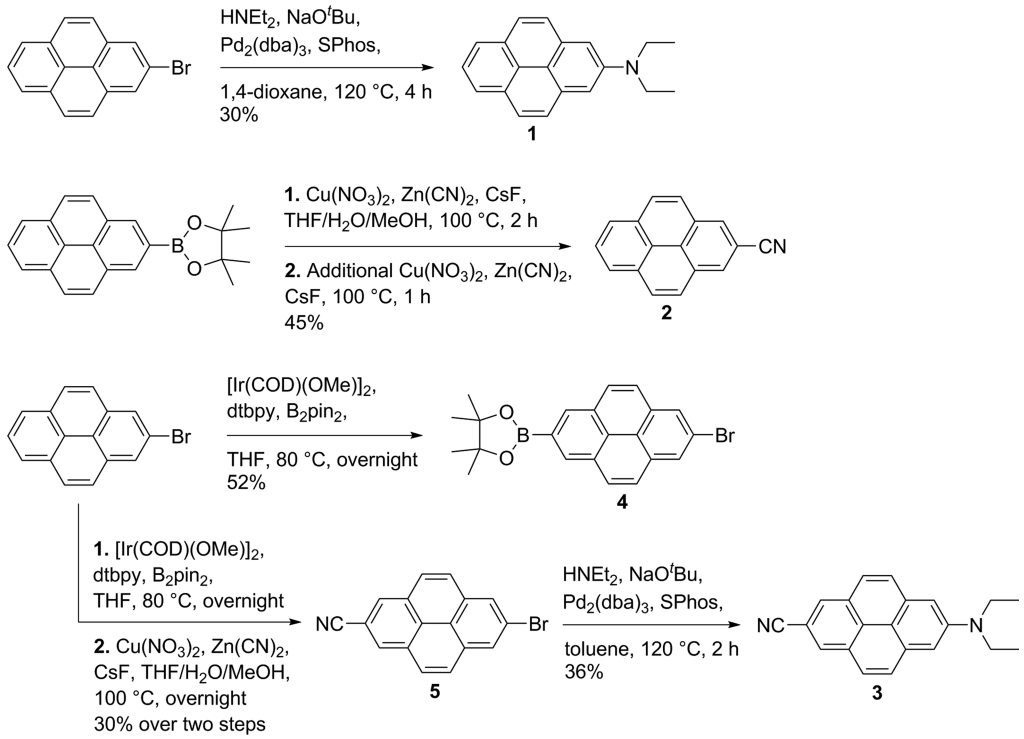

[a]Abbreviations: dba = dibenzylideneacetone; SPhos = 2-dicyclohexylphosphino-2′,6′-dimethoxybiphenyl; COD = 1,5-cyclooctadiene; dtbpy = 4,4′-di-*tert*-butyl-2,2′-bipyridine; pin = pinacolato, $Me_2C(O^-)C(O^-)Me_2$).

DOI: 10.1021/acs.joc.5b00618
J. Org. Chem. 2015, 80, 5658−5665

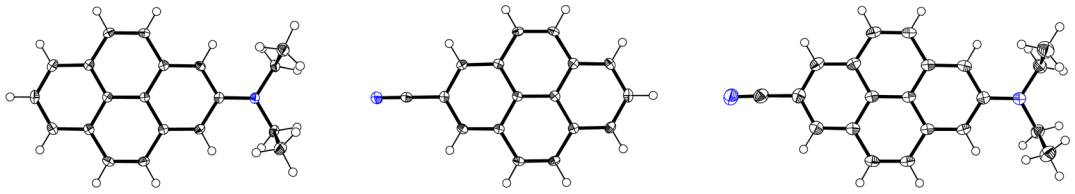

Figure 1. Molecular structures of **1**–**3**, as determined by single-crystal X-ray diffraction. Atom (color): hydrogen (white); carbon (black); nitrogen (blue). Atomic displacement ellipsoids shown at the 50% probability level. See Table S1 for crystallographic data.

Table 1. Photophysical Properties of 1–3 Under an Atmosphere of Argon, Unless Stated Otherwise[a]

	λ_{abs}/nm ($\varepsilon/10^3$ M^{-1} cm^{-1})	medium	λ_{em}/nm	τ/ns	Φ	τ_0/ns	$k_r/10^7$ s^{-1}	$k_{nr}/10^7$ s^{-1}
1	427 (2.8), 341 (27), 285 (80)	Hexane	430	15.2 (Air)/34.3	0.24 (Air)/0.86	40	2.5	0.42
		THF	456	25.1	0.57	44	2.3	1.7
		MeCN	468	21.3	0.42	51	2.0	2.7
		Solid	512	–	–	–	–	–
2	388 (2.0), 335 (37), 257 (68)	Hexane	388	17.6 (Air)/107	0.12 (Air)/0.78	140	0.71	0.20
		THF	392	73.7	0.83	89	1.1	0.23
		MeCN	393	69.0	0.89	78	1.3	0.16
		Solid	455, 482	–	–	–	–	–
3	437 (1.9), 342 (18), 306 (120)	Hexane	440	16.9 (Air)/35.5	0.20 (Air)/0.55	65	1.5	1.3
		THF	473	20.1	0.33	61	1.6	3.3
		MeCN	486	14.5	0.22	66	1.5	5.4
		Solid	498, 531	–	–	–	–	–

[a]The concentration of solution samples was ca. 1×10^{-5} M. Absorption spectra were recorded in hexane solution.

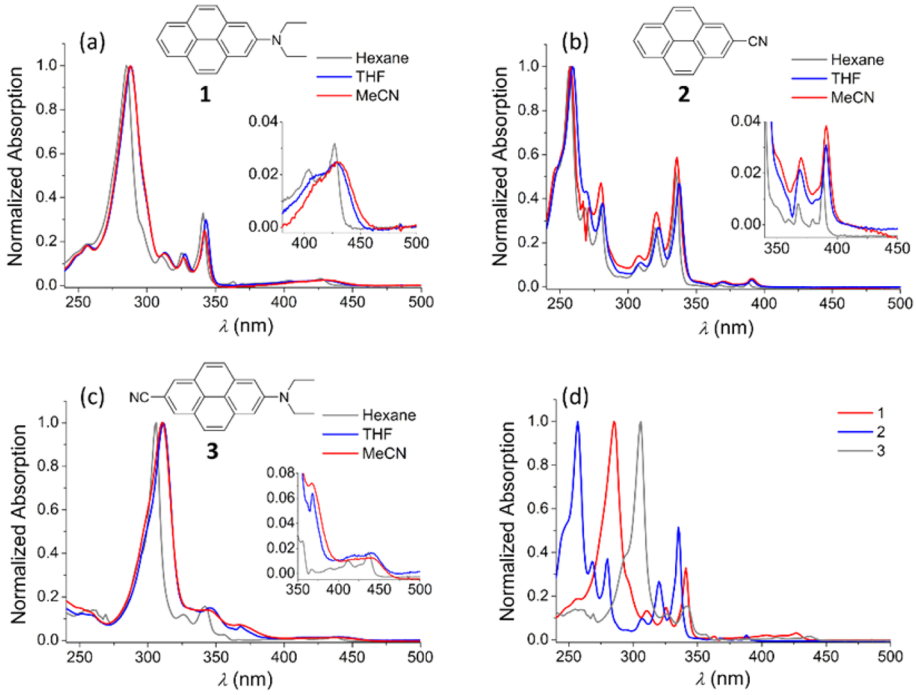

Figure 2. (a–c) UV–visible absorption spectra of compounds **1**–**3** in solvents of different polarity. (d) Comparison of the UV–visible absorption spectra of **1**–**3** in hexane. Insets: Expansions of the $S_1 \leftarrow S_0$ transitions.

stituents through, e.g., orthogonal cross-coupling reactions or conversion of Bpin to a host of other functional groups, such as halides, triflate, alkyl, and alkoxy substituents,[2] or for the synthesis of pyrene-containing polymers via Suzuki-Miyaura coupling. Of mechanistic interest, GC-MS analysis of the crude mixture indicated that trace quantities of other isomers, presumably borylated at the 9- and 10-positions, were present, which, pleasingly from a practical viewpoint, could be removed readily during purification by column chromatography.

Combining the borylation of 2-bromopyrene to give **4** and, in sequence, the procedures for cyanation and amination used in the syntheses of monosubstituted derivatives **2** and **1**, respectively, facilitated the rapid synthesis of **3**. Attempts to isolate the intermediate 2-bromo-7-cyanopyrene (**5**) were

DOI: 10.1021/acs.joc.5b00618
J. Org. Chem. 2015, 80, 5658–5665

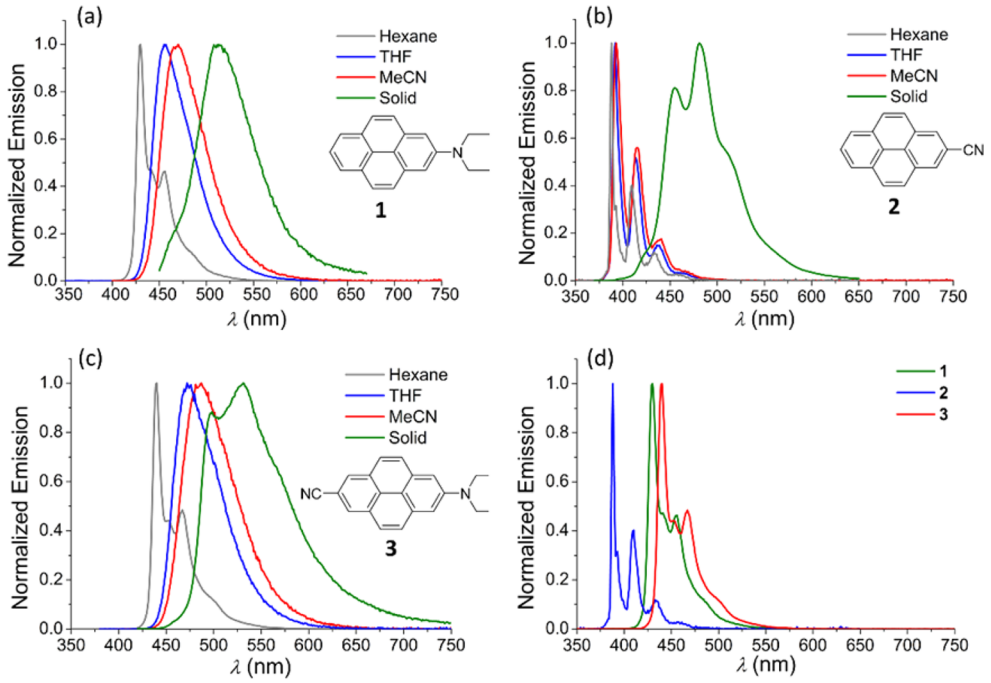

Figure 3. (a–c) Emission spectra of compounds **1**–**3** in solvents of different polarity and in the solid state. (d) Comparison of the emission spectra of **1**–**3** in hexane solutions.

hampered by its low solubility. Only partial purification could be achieved using Soxhlet extraction with toluene over a period of 2 days, followed by column chromatography. Furthermore, it was only possible to obtain a ^{1}H NMR spectrum with an acceptable signal-to-noise ratio for the partially purified compound in hot (72 °C) toluene-d_8. The obtained elemental analysis was low in C content, but acceptable in H and N, while GC-MS demonstrated that only one volatile organic compound was present in solution, and HRMS and ^{1}H NMR were consistent with the proposed structure. We instead found it preferable to synthesize **3** directly without further purification of intermediate **5**, which provided analytically pure **3** in an acceptable isolated yield of 36% and thus nicely demonstrates the potential utility of this approach and of **4** as a versatile reagent.

X-ray Crystal Structures. Compounds **1**–**3** were each investigated by single-crystal X-ray diffraction and their molecular structures are presented in Figure 1. In the solid state, **1** forms head-to-tail π-stacked dimers with an interplanar distance of 3.4360(6) Å and a plane-to-plane centroid offset of 2.7759(8) Å (the planes and centroids are defined by the 16 carbon atoms of the pyrene units). Compound **2** also forms stacks, but within which the molecules lie head-to-head at a distance of 3.4071(9) Å, offset by 3.077(2) Å; neighboring stacks are arranged in a herringbone pattern at an angle of 128.65(2)°. Compound **3** packs in a herringbone motif with no π–π interactions; the planes of the two nearest neighbors (centroid–centroid distance: 5.4227(5) Å) form an angle of 42.25(2)°. The ethyl chains in both structures **1** and **3** adopt a *syn*-conformation with respect to the pyrene plane, which, according to DFT calculations on **3** in the gas phase (optimization at the B3LYP/6-31+G* level), is marginally higher in energy than the *anti*-conformation (ΔE = +0.7 kcal mol^{-1}). The amine in **3** is trigonal planar, which results in a sum of CNC bond angles in the NC_3 plane of 360°. The experimental dihedral angle between the amine NC_3 and arene planes at 100 K is 8.05(4)° (**3**), slightly larger than that reported for DMABN (2.7° at 173 K when measured similarly).[26]

Photophysical Properties. With compounds **1**–**3** in hand, we investigated their solution and solid-state photophysical properties (Table 1). The absorption spectra of each compound in three solvents of increasing polarity (hexane, THF, and MeCN) are shown in Figure 2. Compound **1** exhibits a broad and relatively weak $S_1 \leftarrow S_0$ absorption band in MeCN that has a high-energy shoulder in THF and is well resolved in hexane (ε = 2800 M^{-1} cm^{-1}). By analogy with pyrene, this can be attributed to the short-axis-polarized ^1L_b transition, but includes a contribution of charge transfer from the amine to pyrene in polar solvents. The more intense $S_2 \leftarrow S_0$ (long-axis-polarized ^1L_a transition, ε = 27 000 M^{-1} cm^{-1}) and likely overlapping $S_3 \leftarrow S_0$ and $S_4 \leftarrow S_0$ bands (^1B_b and ^1B_a, respectively, ε = 80 000 M^{-1} cm^{-1}) are also assigned by comparison with pyrene. The absorption spectrum of **2** is the least sensitive to solvent polarity, including the ^1L_b transition, which maintains its structure in all solvents used. Both the ^1L_b and ^1L_a transitions of **3** broaden in polar solvents due to charge transfer. The overlapping ^1B_b and ^1B_a bands are the most significantly shifted among the three derivatives (λ_{max} in the order **2** < **1** < **3**), as can be seen in Figure 2d, and are particularly intense for **3** (120 000 M^{-1} cm^{-1} at 306 nm). The analogous transitions for the parent compound pyrene involve orbitals, viz., the HOMO−1 and LUMO+1, that have significant contributions at the 2,7-positions, i.e., the sites of substitution, and thus it is reasonable that this band is particularly affected by the different substituents. The weak influence of solvent polarity on the absorption spectra of the three compounds, especially **2**, indicates that the ground states are not particularly susceptible to stabilization by solvation in a polar medium.

All three compounds display emission with a high quantum yield in degassed hexane solution (Φ_f = 0.86, 0.78, and 0.55 for

DOI: 10.1021/acs.joc.5b00618
J. Org. Chem. 2015, 80, 5658–5665

1, **2**, and **3**, respectively). The emission spectrum of **1** is well resolved in hexane solution, but is broad and featureless in THF and MeCN solutions with a solvatochromic shift of up to 1920 cm^{-1}, indicating that the emission is from a $\pi-\pi^*$ state in a nonpolar environment and from a state of greater charge-transfer character in more polar solvents. In contrast, the emission of **2** is more weakly solvatochromic, shifting only 330 cm^{-1} from hexane to MeCN solutions. It exhibits sharp, well-resolved emission in all three solvents with an average vibrational spacing between the most prominent bands of ca. 1350 cm^{-1} (assigned to an average of aromatic ring vibrational modes), and thus a pure $\pi-\pi^*$ description is appropriate for the emission in all solvents studied. This is also revealed by its long pure-radiative lifetime, τ_0, in hexane solution of 140 ns. The emission of **3** is similar to that of **1**, albeit slightly red-shifted (530 cm^{-1} in hexane solution) and with an increased maximum solvatochromic shift of 2100 cm^{-1}. The pure radiative lifetimes of these two compounds are also similar (τ_0 = 40 ns (**1**) and 65 ns (**3**) in hexane solutions) with little solvent dependence. Furthermore, **1** and **3** have shorter τ_0 values than **2** in hexane solution; the τ_0 value of **2** also has a moderate solvent dependence, shortening to 78 ns in MeCN solution. Compound **2** has excellent quantum yields in all solvents, having a value as high as 0.89 in MeCN solution; this is attributable to its low and almost solvent independent nonradiative decay rate, k_{nr}, while having a larger, only weakly solvent dependent radiative rate, k_r. Even though increased nonradiative decay leads to somewhat quenched emission for **1** and **3** in more polar solvents, moderately high quantum yields of 0.42 (**1**) and 0.22 (**3**) are still achieved in MeCN solutions. While the amino substituent clearly affects the orbital structure of pyrene, such that charge transfer becomes feasible, the cyano group is poorly conjugated and serves only to make the pyrene slightly more electron accepting. These conclusions are broadly in accord with theoretical calculations, vide infra.

In the solid state, the emission maxima of all three compounds are red-shifted relative to any of the solution samples, most notably for **2** (Figure 3). While the emission of **1** is structureless, that of **2** exhibits two vibronic bands and a low-energy shoulder; this would suggest different origins of the emission, although this is not clear at present. For **3**, the spectral shape can be described as a hybrid of that of **1** and **2**. Possible reasons for the strong red shift in emission relative to the solution state include excimer formation, leading to broadened emission, and excitonic aggregate emission.

None of the compounds showed excimer emission in more concentrated hexane solutions (ca. 2×10^{-3} M for **1**; saturated at 5×10^{-4} M for **2** and **3**), while exciplex formation between **2** and *N*,*N*-dimethylaniline (ca. 0.2 M in hexane) could be observed. The broad emission from this exciplex is centered at 474 nm and is shifted bathochromically by ca. 1370 cm^{-1} from that observed from the pyrene:*N*,*N*-diethylaniline exciplex in hexane at ca. 445 nm.[27−29]

The known compounds DMABN and 2-cyano-7-(*N*,*N*-dimethylamino)-4,5,9,10-tetrahydropyrene[30] (**6**) (Scheme 3) are good model systems with which to compare the photophysical behavior of **3**. Compound **6** has been reported to show solvent-dependent emission, with a change of band shape from structured to broad upon increasing solvent polarity, which was interpreted as a change from a locally excited $\pi-\pi^*$ state to an intramolecular charge transfer (ICT) state. The emission solvatochromism of **6** (ca. 3900 cm^{-1} shift in λ_{max} between cyclohexane and MeCN solutions) is more

Scheme 3. Compounds DMABN and 2-Cyano-7-(*N*,*N*-dimethylamino)-4,5,9,10-tetrahydropyrene (6) Reported by Sumalekshmy and Gopidas[30]

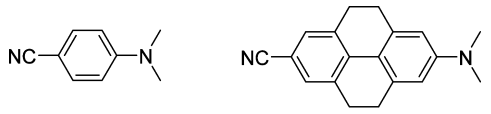

DMABN 6

pronounced than that of **3**. Thus, although 2,7-substituted pyrene evidently can act as a reasonable π-bridge for constructing donor−acceptor systems, facilitating charge transfer in the excited state with suitable substituents, it is not as proficient as 2,7-substituted 4,5,9,10-tetrahydropyrene. However, such tempered conjugation between a donor and acceptor unit has been suggested to be desirable in some applications, such as dye-sensitized solar cells, because it may hinder charge recombination.[31] The related compound DMABN is also known to show solvent-dependent dual emission from locally excited and TICT states; however, no such phenomenon was observed for **3**, and thus we conclude that **3** does not form a low-energy TICT state in polar solvents.

Computational Modeling. DFT and TD-DFT studies of **1**−**3** were conducted to aid the assignment of the spectral data (Figure 4). The ground-state structures were first optimized in

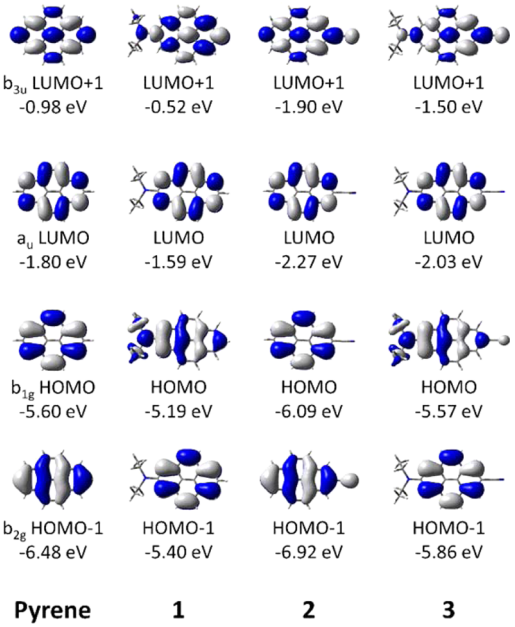

Figure 4. DFT-calculated orbitals of **1**−**3** (B3LYP/6-31+G*, gas phase). Surface isovalue: ± 0.02 $[e\ a_0^{-3}]^{1/2}$.

the gas-phase using the B3LYP/6-31+G* level of theory.[32−34] Compound **2** has been studied theoretically previously (DFT optimization with B3LYP/6-31+G*), and the molecular structure and orbital scheme are in agreement with those presented herein. The optimized geometries obtained are also in good agreement with the experimental structures determined by X-ray crystallography in terms of bond lengths and, for **1** and **3**, the dihedral angles between the NC_3 and pyrene mean planes. Furthermore, the structure of **3** was optimized in solution using the conductor-like polarizable continuum model (CPCM) to simulate the limiting cases of hexane and MeCN. TD-DFT calculations were performed at the obtained gas-

DOI: 10.1021/acs.joc.5b00618
J. Org. Chem. 2015, 80, 5658−5665

phase and solution geometries using both the B3LYP and CAM-B3LYP functionals, due to a known problem of obtaining the correct ordering of excited states of the parent compound pyrene with the former[35] and the resolution of this problem with the latter,[3] and the 6-31+G* double-ζ basis set (Figures S16−S25; Tables S2−S10).

For pyrene, the $S_1 \leftarrow S_0$ transition is described by a nearly 50:50 weighted combination of LUMO ← HOMO−1 and LUMO+1 ← HOMO; thus, these are the four key orbitals that need to be considered in any discussion of the optical properties of pyrene derivatives. For the amine-containing compounds **1** and **3**, the nitrogen centered $2p_z$ orbital (lone-pair) of the NEt_2 fragment mixes with the b_{2g}-symmetry HOMO−1 of the pyrene fragment that has a contribution at the 2-position. The orbital thus formed in the case of **1** is 1.29 eV higher in energy than the HOMO−1 of pyrene, which is significantly more destabilized than the HOMO of pyrene, originally of b_{1g} symmetry, that is raised by only 0.20 eV, leading to a switch in their ordering. This makes the amine a good donor group, and introduces charge transfer character to the S_1 excited state. The a_u-symmetry LUMO of pyrene does not mix well with the amine-fragment orbitals, resulting in only a 0.21 eV increase in energy. Mixing with the b_{3u}-symmetry LUMO+1 of pyrene does have a greater effect though, as it has a significant contribution at the 2-position; this orbital is destabilized by 0.46 eV. In contrast, although the acceptor CN fragment has the correct symmetry to mix with the b_{3u}-symmetry LUMO+1 of pyrene, it does not mix sufficiently well to lower its energy below that of the pyrene a_u-symmetry LUMO (stabilized by 0.92 and 0.47 eV, respectively); thus, the cyano group is a relatively ineffective acceptor group when substituted at the 2-position of pyrene. This is reflected in the photophysical behavior of **2**, which is only mildly perturbed from that of pyrene and shows little solvatochromism. Compound **3**, containing both of these groups, has clear features of each. The HOMO and HOMO−1 are similar to those of **1** while the LUMO and LUMO+1 are more akin to **2**; the energies of these key orbitals are, in general, intermediate between the appropriate orbitals of **1** and **2**, reflecting the balance of influences of the donor and acceptor group that can be achieved. The short-axis-polarized $S_3 \leftarrow S_0$ transition of **3**, similar to that of pyrene, is the difference combination of LUMO ← HOMO−1 and LUMO+1 ← HOMO, and has a very large oscillator strength, f = 2.03, accounting for the highest intensity bands in the absorption spectra shown in Figure 2a−c. Full results of the TD-DFT calculated transitions from the ground-state optimized geometries for all compounds are presented in the SI, along with simulated absorption spectra.

TD-DFT transition energies of **3** in hexane and MeCN solutions were only slightly perturbed from those in the gas-phase, in line with the small change in absorption maximum observed experimentally upon increasing the solvent polarity. The TD-DFT-optimized S_1 structure of **3** in MeCN showed no evidence for twisting of the amino group to form a TICT geometry (NC_3−pyrene dihedral angles: S_0 5.8°, S_1 3.3°); thus, **3** behaves very differently from DMABN, the classic example of a TICT-state-forming compound. This is readily accounted for by the poorer conjugation between the donor and the acceptor in **3**. The calculated emission wavelengths of 387 and 404 nm in hexane and MeCN solution, respectively, and associated shift (1130 cm^{-1}), reproduce relatively well the experimentally observed emission energies and the bathochromic shift from hexane to MeCN solution (2100 cm^{-1}).

CONCLUSIONS

A method to synthesize 2,7-disubstituted pyrene derivatives having two different substituents is reported that is more selective and general than those described previously. The demonstrated method will be applicable to a wide range of pyrene-based functional materials and will facilitate studies that aim to exploit the unique orbital structure of pyrene to produce compounds with modulated charge transfer. We show that amino substitution at the 2-position of pyrene raises the energy of the HOMO−1 orbital of unsubstituted pyrene through mixing with the nonbonding $2p_z$ orbital of the nitrogen atom, thus removing the nodal plane along the long axis of the molecule in the HOMO. The weak cyano acceptor lowers the energy of the pyrene-like LUMO+1, but it does not lead to a switch in the ordering with the LUMO. Inclusion of even stronger acceptor moieties is expected to do so, and thus careful selection of donor and acceptor moieties in 2,7-disubstituted pyrene derivatives will allow the design of compounds with bespoke electronic properties that can be made readily using the methodology presented herein.

EXPERIMENTAL SECTION

General Experimental Methods. All reagents were obtained from commercial sources and used as received, with the exception of 2-bromopyrene[2] and $[Ir(COD)(\mu\text{-OMe})]_2$,[36] which were synthesized as reported previously. Solvents were HPLC grade, and were treated to remove trace water using a commercial solvent purification system and deoxygenated using the freeze−pump−thaw method. NMR spectra were recorded in $CDCl_3$, CD_2Cl_2, DMSO-d_6, or toluene-d_8 solution on a 500 MHz (^{1}H) spectrometer. ^{1}H NMR spectra are either referenced to TMS directly or via the signal of the residual protiated solvent. $^{13}C\{^1H\}$ NMR spectra are either referenced to TMS directly or via the ^{13}C resonance of the deuterated solvent. ^{11}B NMR spectra are referenced to external $BF_3{\cdot}Et_2O$. MS was performed in EI^+ mode on a GC-MS and HRMS was performed in ESI^+ mode on a μ-TOF mass spectrometer.

2-(*N*,*N*-Diethylamino)pyrene (1). In an argon-filled glovebox, 2-bromopyrene (610 mg, 2.2 mmol), Pd_2dba_3 (9 mg, 0.01 mmol, 0.5 mol %), SPhos (12 mg, 0.029 mmol, 1 mol %), NaO^tBu (580 mg, 6.0 mmol), diethylamine (0.5 mL, 5 mmol), and 1,4-dioxane (8 mL) were added to a Schlenk tube. The tube was then sealed with a PTFE stopcock, taken out of the glovebox, and heated in an oil bath at 120 °C for 4 h, until GC-MS monitoring indicated that the reaction was complete. The solution was cooled to r.t., and the solvent and volatiles were removed in vacuo. Purification was performed by column chromatography (basic Al_2O_3; 1:3 CH_2Cl_2/pentane). Recrystallization by layer diffusion of methanol into a CH_2Cl_2 solution gave the title compound as a yellow crystalline solid (185 mg, 30%). ^{1}H NMR (CD_2Cl_2, 500 MHz): δ = 8.06 (d, J = 8 Hz, 2 H), 7.96 (d, J = 9 Hz, 2 H), 7.91 (d, J = 9 Hz, 2 H), 7.83−7.80 (m, 1 H), 7.49 (s, 2 H), 3.63 (q, J = 7 Hz, 4 H), 1.32 (t, J = 7 Hz, 6 H) ppm. $^{13}C\{^1H\}$ NMR (CD_2Cl_2, 125 MHz): δ = 147.1, 133.0, 130.0, 127.7, 127.3, 125.3, 125.2, 124.2, 117.3, 109.1, 45.1, 12.8 ppm. Anal. Calcd for $C_{20}H_{19}N$: C 87.87, H 7.01, N 5.12; Found: C 88.16, H 7.02, N 5.27. MS (EI^+): m/z = 273 [M^+].

2-Cyanopyrene (2). In a two-neck round-bottom flask fitted with a reflux condenser, 2-(Bpin)pyrene (328 mg, 1.0 mmol) was dissolved in hot methanol (50 mL), to which $Zn(CN)_2$ (400 mg, 3.4 mmol) and CsF (200 mg, 1.3 mmol) were added. The suspension was heated to reflux with stirring in an oil bath, and a solution of $Cu(NO_3)_2{\cdot}3H_2O$ (500 mg, 2.1 mmol) in water (20 mL) was added dropwise. The temperature was then increased to 100 °C. After 2 h, GC-MS showed the reaction mixture to contain predominantly the product 2-cyanopyrene, with residual 2-(Bpin)pyrene and protodeborylated

DOI: 10.1021/acs.joc.5b00618
J. Org. Chem. 2015, 80, 5658−5665

starting material (pyrene). Additional $Zn(CN)_2$ (400 mg, 3.4 mmol), CsF (200 mg, 1.3 mmol), and a solution of $Cu(NO_3)_2 \cdot 3H_2O$ (500 mg, 2.1 mmol) in water (20 mL) were then added to the solution. The reaction mixture was heated for another 1 h. GC-MS showed the reaction to be nearly complete with only traces of 2-(Bpin)pyrene left. After cooling to room temperature, water (100 mL) was added, and the suspension was extracted with CH_2Cl_2 (3 × 200 mL). The organic layer was separated, dried over Na_2SO_4, and filtered. The solvents were removed in vacuo, and the residue was purified by column chromatography (SiO_2; 1:1 CH_2Cl_2/pentane) to give the title compound as a colorless solid. The product was recrystallized from methanol as white needles (102 mg, 45%). ^{1}H NMR ($CDCl_3$, 500 MHz) δ = 8.38 (s, 2 H), 8.26 (d, J = 8 Hz, 2 H), 8.16 (d, J = 9 Hz, 2 H), 8.13−8.19 (m, 1 H), 8.04 (d, J = 9 Hz, 2 H) ppm. ^{13}C{^{1}H} NMR ($CDCl_3$, 125 MHz) δ = 131.7, 131.4, 129.4, 127.7, 127.5, 126.7, 126.33, 126.32, 123.9, 119.8, 109.3 ppm. Anal. Calcd for $C_{17}H_9N$: C 89.85, H 3.99, N 6.16; Found: C 89.95, H 4.03, N 6.14. MS (EI$^+$): m/z 227 [M$^+$].

2-Cyano-7-(*N*,*N*-diethylamino)pyrene (3). In an argon-filled glovebox, 2-bromo-7-cyanopyrene (**5**) (103 mg, 0.33 mmol), Pd_2dba_3 (3 mg, 0.003 mmol, 1 mol %), SPhos (4 mg, 0.01 mmol, 3 mol %), NaO^{t}Bu (120 mg, 1.2 mmol), diethylamine (0.2 mL, 2 mmol), and toluene (4 mL) were added to a Schlenk tube. The tube was sealed with a PTFE stopcock, taken out of the glovebox and heated at 120 °C in an oil bath for 2 h, until GC-MS monitoring indicated that the reaction was complete. After removing the solvent and volatiles in vacuo, the residue was purified by automated flash chromatography (KP-silica, 0:1 to 1:0 CH_2Cl_2/hexane gradient in a total of 10 column volumes). The product was then recrystallized by slow evaporation of a 1:1 CH_2Cl_2/hexane solution under argon to give the title compound as yellow plates (36 mg, 36%). ^{1}H NMR (DMSO-d_6, 500 MHz): δ = 8.53 (s, 2 H), 8.13 (d, J = 9 Hz, 2 H), 8.06 (d, J = 9 Hz, 2 H), 7.66 (s, 2 H), 3.63 (q, J = 7 Hz, 4 H), 1.26 (t, J = 7 Hz, 6 H) ppm. ^{13}C{^{1}H} NMR (CD_2Cl_2, 125 MHz): δ = 148.2, 133.6, 129.9, 129.0, 127.7, 127.0, 126.8, 120.5, 116.2, 109.7, 106.9, 45.2, 12.7 ppm. Anal. Calcd for $C_{21}H_{18}N_2$: C 84.53, H 6.08, N 9.39; Found: C 84.11, H 6.33, N 9.44. MS (EI$^+$): m/z = 298 [M$^+$].

2-Bpin-7-bromopyrene (4). In an argon-filled glovebox, 2-bromopyrene (2.00 g, 7.1 mmol), B_2pin_2 (2.06 g, 8.1 mmol), 4,4′-di-*tert*-butyl-2,2′-bipyridine (dtbpy) (24 mg, 0.089 mmol, 1.2 mol %), $[Ir(COD)(\mu\text{-OMe})]_2$ (27 mg, 0.041 mmol, 0.6 mol %), and THF (20 mL) were added to a Schlenk tube. The tube was sealed with a PTFE stopcock and heated at 80 °C in an oil bath overnight. After removal of the solvent in vacuo, the residue was purified by column chromatography (SiO_2; 1:4 CH_2Cl_2/hexane), followed by recrystallization from hexane solution to give the title compound as colorless needles (1.5 g, 52%). ^{1}H NMR ($CDCl_3$, 500 MHz): δ = 8.65 (s, 2 H), 8.25 (s, 2 H), 8.11 (d, J = 9 Hz, 2 H), 7.94 (d, J = 9 Hz, 2 H), 1.47 (s, 12 H) ppm. ^{13}C{^{1}H} NMR ($CDCl_3$, 125 MHz): δ = 133.3, 132.2, 130.2, 129.2, 127.1, 126.3, 126.1, 123.3, 120.6, 84.4, 25.2 ppm (one C not observed, likely that attached to B). ^{11}B NMR (161 MHz, $CDCl_3$): δ = 30.5 ppm. Anal. Calcd for $C_{22}H_{20}BO_2Br$: C 64.91, H 4.95; Found: C 64.97, H 5.03. MS (EI$^+$): m/z = 406 [M$^+$].

2-Bromo-7-cyanopyrene (5). In an argon-filled glovebox, 2-bromopyrene (740 mg, 2.6 mmol), B_2pin_2 (762 mg, 3.0 mmol), dtbpy (8 mg, 0.03 mmol, 1 mol %), $[Ir(COD)(\mu\text{-OMe})]_2$ (9 mg, 0.01 mmol, 0.5 mol %), and THF (10 mL) were added to a Schlenk tube. The tube was sealed with a PTFE stopcock and heated at 80 °C in an oil bath overnight. After removing the solvent in vacuo, the residue was dissolved in a mixture of THF (15 mL) and methanol (10 mL). A suspension of $Zn(CN)_2$ (1.05 g, 9.1 mmol), CsF (456 mg, 3.0 mmol), and $Cu(NO_3)_2 \cdot 3H_2O$ (1.46 g, 6.1 mmol) in water (15 mL) was then added. The reaction mixture was heated at 100 °C overnight. The crude mixture was extracted with toluene in a Soxhlet extractor over a period of 2 d. The extract was adsorbed onto silica, and further purification was achieved by column chromatography (SiO_2; 1:1 CH_2Cl_2/hexane), affording the title compound as an off-white powder (280 mg, 30%). The solubility of this compound is too low to allow complete purification or to obtain a ^{13}C{^{1}H} NMR spectrum of suitable signal-to-noise ratio. The signals of the ^{1}H NMR spectrum of this compound are very weak, even in toluene-d_8 at 72 °C. GC-MS indicated the presence of a single volatile product (see the SI). ^{1}H NMR (toluene-d_8, 72 °C, 500 MHz): δ = 7.97 (s, 2 H), 7.77 (s, 2 H), 7.47 (d, J = 9 Hz, 2 H), 7.45 (d, J = 9 Hz, 2 H) ppm. Anal. Calcd for $C_{17}H_8BrN$: C 66.69, H 2.63, N 4.58; Found: C 65.76, H 2.37, N 4.96. MS (EI$^+$): m/z = 305 [M$^+$]. HRMS (ESI$^+$): Calcd for $C_{17}H_8BrN^+$ m/z = 304.98346; Found 304.98343 [M$^+$] (|$\Delta m/z$| = 0.11 ppm).

X-ray Crystallography. Crystals suitable for single-crystal X-ray diffraction were selected, coated with perfluoropolyether oil, and mounted on sample holders. The diffraction experiments were carried out with Mo Kα radiation while the sample was constantly cooled in a stream of nitrogen at 100 K and the data were collected with a CCD area detector. Using the software package OLEX2,[37] the structures were solved with the XS structure solution program[38] using direct methods and refined with the XL refinement package[38] using least-squares minimizations. The 0 1 1 (**1** and **2**) and 0 2 0 (**1**) reflections were obscured by the beam stop and were, therefore, omitted from the refinements. CCDC-1052639 (**1**), 1052640 (**2**), and 1052641 (**3**) contain the supplementary crystallographic data for this paper. These data can be obtained free of charge from The Cambridge Crystallographic Data Centre via www.ccdc.cam.ac.uk/data_request/cif.

Theoretical Methods. All calculations (DFT and TD-DFT) were carried out with the program package *Gaussian 09* (rev. D.01).[39] The ground-state geometries were optimized without symmetry constraints using the B3LYP[32,33] functional in combination with the 6-31+G* basis set.[34] The molecular structures obtained from single-crystal X-ray diffraction of **1**, **2**, and **3** were used as the starting geometries. The optimized geometries were confirmed to be local minima by performing frequency calculations and obtaining only positive (real) frequencies. These solutions were additionally checked for wave function stability. Based on these optimized structures, the lowest-energy gas-phase vertical transitions were calculated (singlets, 25 states) by TD-DFT using both B3LYP and the Coulomb-attenuated functional CAM-B3LYP[40] in combination with the 6-31+G* basis set, as this pairing has been shown to be effective for both pyrene and ICT systems.[41] No symmetry constraints were used in any of the calculations. Solvent effects were included using the conductor-like polarizable continuum model (CPCM) with united-atom Kohn−Sham (UAKS) sphere radii and the appropriate dielectric constant for the considered solvent. The structures of S_1 states were optimized at the CAM-B3LYP/6-31+G(d) level.

Photophysical Measurements. All solution-state measurements were made in standard quartz cuvettes (1 cm × 1 cm cross-section). UV−visible absorption spectra were recorded using a diode array UV−visible spectrophotometer. The emission spectra were recorded on a spectrometer equipped with a double monochromator for both excitation and emission, operating in right-angle geometry mode. All spectra were fully corrected for the spectral response of the instrument. All solutions used in photophysical measurements had a concentration of ca. 1×10^{-5} M, except where stated. The fluorescence quantum yields were measured using a calibrated integrating sphere (150 mm inner diameter). For solution-state measurements, the longest-wavelength absorption maximum of the compound in the respective solvent was chosen as the excitation wavelength, while for solid-state measurements, the longest-wavelength absorption maximum in hexane was selected. Fluorescence lifetimes were recorded using the time-correlated single-photon counting (TCSPC) method. Solutions were excited with either a 374 nm pulsed diode laser (**1** and **3**) or a 275 nm pulsed LED (**2**) at repetition rates of 1−5 MHz and were recorded at the emission maxima. The instrument response functions (IRF) were ca. 950 ps fwhm. Decays were recorded to 10 000 counts in the peak channel with a record length of at least 1000 channels. The band-pass of the monochromator was adjusted to give a signal count rate of <20 kHz. Iterative reconvolution of the IRF with one decay function and nonlinear least-squares analysis were used to analyze the data. The quality of all decay fits was judged to be satisfactory based on the calculated values of the reduced χ^2 and Durbin-Watson parameters and visual inspection of the weighted and autocorrelated residuals.

DOI: 10.1021/acs.joc.5b00618
J. Org. Chem. 2015, 80, 5658−5665

■ ASSOCIATED CONTENT

Supporting Information

Copies of NMR spectra and GC-MS traces and spectra, Cartesian coordinates of DFT-optimized structures and further TD-DFT results, including simulated absorption spectra, and X-ray crystallographic data in CIF format for **1**−**3**. The Supporting Information is available free of charge on the ACS Publications website at DOI: 10.1021/acs.joc.5b00618.

■ AUTHOR INFORMATION

Corresponding Authors

*E-mail: robert.edkins@uni-wuerzburg.de.

*E-mail: todd.marder@uni-wuerzburg.de.

Notes

The authors declare no competing financial interest.

■ ACKNOWLEDGMENTS

We are grateful for generous financial support by the Bavarian State Ministry of Science, Research, and the Arts for the Collaborative Research Network "Solar Technologies go Hybrid". R.M.E. and A.L. thank the Alexander von Humboldt Foundation for Postdoctoral Research Fellowships. T.B.M. thanks AllyChem Co. Ltd. for a generous gift of B_2pin_2.

■ REFERENCES

(1) Figueira-Duarte, T. M.; Müllen, K. *Chem. Rev.* **2011**, *111*, 7260.

(2) Crawford, A. G.; Liu, Z.; Mkhalid, I. A. I.; Thibault, M.-H.; Schwarz, N.; Alcaraz, G.; Steffen, A.; Collings, J. C.; Batsanov, A. S.; Howard, J. A. K.; Marder, T. B. *Chem.—Eur. J.* **2012**, *18*, 5022.

(3) Crawford, A. G.; Dwyer, A. D.; Liu, Z.; Steffen, A.; Beeby, A.; Pålsson, L.-O.; Tozer, D. J.; Marder, T. B. *J. Am. Chem. Soc.* **2011**, *133*, 13349.

(4) Mkhalid, I. A. I.; Barnard, J. H.; Marder, T. B.; Murphy, J. M.; Hartwig, J. F. *Chem. Rev.* **2009**, *110*, 890.

(5) Coventry, D. N.; Batsanov, A. S.; Goeta, A. E.; Howard, J. A. K.; Marder, T. B.; Perutz, R. N. *Chem. Commun.* **2005**, 2172.

(6) Casas-Solvas, J. M.; Howgego, J. D.; Davis, A. P. *Org. Biomol. Chem.* **2014**, *12*, 212.

(7) Zhang, S.; Qiao, X.; Chen, Y.; Wang, Y.; Edkins, R. M.; Liu, Z.; Li, H.; Fang, Q. *Org. Lett.* **2014**, *16*, 342.

(8) Edkins, R. M.; Fucke, K.; Peach, M. J. G.; Crawford, A. G.; Marder, T. B.; Beeby, A. *Inorg. Chem.* **2013**, *52*, 9842.

(9) Foster, J. A.; Edkins, R. M.; Cameron, G. J.; Colgin, N.; Fucke, K.; Ridgeway, S.; Crawford, A. G.; Marder, T. B.; Beeby, A.; Cobb, S. L.; Steed, J. W. *Chem.—Eur. J.* **2014**, *20*, 279.

(10) Batsanov, A. S.; Howard, J. A. K.; Albesa-Jové, D.; Collings, J. C.; Liu, Z.; Mkhalid, I. A. I.; Thibault, M.-H.; Marder, T. B. *Cryst. Growth Des.* **2012**, *12*, 2794.

(11) Liu, Z.; Wang, Y.; Chen, Y.; Liu, J.; Fang, Q.; Kleeberg, C.; Marder, T. B. *J. Org. Chem.* **2012**, *77*, 7124.

(12) Ji, L.; Fucke, K.; Bose, S. K.; Marder, T. B. *J. Org. Chem.* **2015**, *80*, 661.

(13) Eliseeva, M. N.; Scott, L. T. *J. Am. Chem. Soc.* **2012**, *134*, 15169.

(14) Li, S.-S.; Jiang, K.-J.; Yu, C.-C.; Huang, J.-H.; Yang, L.-M.; Song, Y.-L. *New J. Chem.* **2014**, *38*, 4404.

(15) Fu, P. P.; Lee, H. M.; Harvey, R. G. *J. Org. Chem.* **1980**, *45*, 2797.

(16) Lee, H.; Harvey, R. G. *J. Org. Chem.* **1986**, *51*, 2847.

(17) Lippert, E.; Lüder, W.; Boos, H. In *Advances in Molecular Spectroscopy*, Proceedings of the IVth International Conference on Molecular Spectroscopy, 1959; Mangini, A., Ed.; Pergamon Press: Oxford, 1962; pp 443−457.

(18) Rettig, W. *Angew. Chem., Int. Ed. Engl.* **1986**, *25*, 971.

(19) Grabowski, Z. R.; Rotkiewicz, K.; Rettig, W. *Chem. Rev.* **2003**, *103*, 3899.

(20) Pigliucci, A.; Vauthey, E.; Rettig, W. *Chem. Phys. Lett.* **2009**, *469*, 115.

(21) Coto, P. B.; Serrano-Andres, L.; Gustavsson, T.; Fujiwara, T.; Lim, E. C. *Phys. Chem. Chem. Phys.* **2011**, *13*, 15182.

(22) Rhinehart, J. M.; Challa, J. R.; McCamant, D. W. *J. Phys. Chem. B* **2012**, *116*, 10522.

(23) Catalan, J. *Phys. Chem. Chem. Phys.* **2013**, *15*, 8811.

(24) Park, M.; Kim, C. H.; Joo, T. *J. Phys. Chem. A* **2013**, *117*, 370.

(25) Liskey, C. W.; Liao, X.; Hartwig, J. F. *J. Am. Chem. Soc.* **2010**, *132*, 11389.

(26) Jameson, G. B.; Sheikh-Ali, B. M.; Weiss, R. G. *Acta Crystallogr.* **1994**, *B50*, 703.

(27) Mataga, N.; Okada, T.; Ezumi, K. *Mol. Phys.* **1966**, *10*, 203.

(28) Mataga, N.; Okada, T.; Oohari, H. *Bull. Chem. Soc. Jpn.* **1966**, *39*, 2563.

(29) Mataga, N.; Okada, T.; Yamamoto, N. *Chem. Phys. Lett.* **1967**, *1*, 119.

(30) Sumalekshmy, S.; Gopidas, K. R. *J. Phys. Chem. B* **2004**, *108*, 3705.

(31) Maggio, E.; Martsinovich, N.; Troisi, A. *Angew. Chem., Int. Ed.* **2013**, *52*, 973.

(32) Becke, A. D. *J. Chem. Phys.* **1993**, *98*, 5648.

(33) Lee, C.; Yang, W.; Parr, R. G. *Phys. Rev. B* **1988**, *37*, 785.

(34) Hehre, W. J.; Ditchfield, R.; Pople, J. A. *J. Chem. Phys.* **1972**, *56*, 2257.

(35) Parac, M.; Grimme, S. *Chem. Phys.* **2003**, *292*, 11.

(36) Uson, R.; Oro, L. A.; Cabeza, J. A.; Bryndza, H. E.; Stepro, M. P. *Inorg. Synth.* **1985**, *23*, 126.

(37) Dolomanov, O. V.; Bourhis, L. J.; Gildea, R. J.; Howard, J. A. K.; Puschmann, H. *J. Appl. Crystallogr.* **2009**, *42*, 339.

(38) Sheldrick, G. *Acta Crystallogr.* **2008**, *A64*, 112.

(39) Frisch, M. J.; Trucks, G. W.; Schlegel, H. B.; Scuseria, G. E.; Robb, M. A.; Cheeseman, J. R.; Scalmani, G.; Barone, V.; Mennucci, B.; Petersson, G. A.; Nakatsuji, H.; Caricato, M.; Li, X.; Hratchian, H. P.; Izmaylov, A. F.; Bloino, J.; Zheng, G.; Sonnenberg, J. L.; Hada, M.; Ehara, M.; Toyota, K.; Fukuda, R.; Hasegawa, J.; Ishida, M.; Nakajima, T.; Honda, Y.; Kitao, O.; Nakai, H.; Vreven, T.; Montgomery, J. A.; Peralta, J. E.; Ogliaro, F.; Bearpark, M.; Heyd, J. J.; Brothers, E.; Kudin, K. N.; Staroverov, V. N.; Kobayashi, R.; Normand, J.; Raghavachari, K.; Rendell, A.; Burant, J. C.; Iyengar, S. S.; Tomasi, J.; Cossi, M.; Rega, N.; Millam, J. M.; Klene, M.; Knox, J. E.; Cross, J. B.; Bakken, V.; Adamo, C.; Jaramillo, J.; Gomperts, R.; Stratmann, R. E.; Yazyev, O.; Austin, A. J.; Cammi, R.; Pomelli, C.; Ochterski, J. W.; Martin, R. L.; Morokuma, K.; Zakrzewski, V. G.; Voth, G. A.; Salvador, P.; Dannenberg, J. J.; Dapprich, S.; Daniels, A. D.; Farkas, Ö.; Foresman, J. B.; Ortiz, J. V.; Cioslowski, J.; Fox, D. J. *Gaussian 09*, revision D.01; Gaussian, Inc., Wallingford, CT, 2009.

(40) Yanai, T.; Tew, D. P.; Handy, N. C. *Chem. Phys. Lett.* **2004**, *393*, 51.

(41) Peach, M. J. G.; Benfield, P.; Helgaker, T.; Tozer, D. J. *J. Chem. Phys.* **2008**, *128*, 044118.

DOI: 10.1021/acs.joc.5b00618
J. Org. Chem. 2015, 80, 5658−5665